How to Cite:
Anitha, D., & Priya, S. S. (2022). An enhanced anarchic society optimization technique for the classification of ultrasound thyroid images using ILBP. *International Journal of Health Sciences*, *6*(S2), 4713–4722. https://doi.org/10.53730/ijhs.v6nS2.6125

An enhanced anarchic society optimization technique for the classification of ultrasound thyroid images using ILBP

Dr. D. Anitha
Associate Professor, Sri Ramakrishna College of Art & Science for Women, Coimbatore, Tamil Nadu, India. Research Scholar, Sri Ramakrishna College of Art & Science for Women, Coimbatore, Tamil Nadu, India
Email: anithacs@srcw.ac.in

S. Sathya Priya
Associate Professor, Sri Ramakrishna College of Art & Science for Women, Coimbatore, Tamil Nadu, India. Research Scholar, Sri Ramakrishna College of Art & Science for Women, Coimbatore, Tamil Nadu, India
Email: sathyanetra@gmail.com

***Abstract*---**In the recent times, Thyroid Nodules (TNs) is a generic cancer of the thyroid gland, which impacts close to 20% of the population worldwide and nearly 50% of 60- year-old individuals. The conventional diagnostic method, relying on the expertise of doctors, shows a huge drawback that the diagnosis result very much relies on the individual knowledge and experience of the physician. As a result, efficacy of diagnosis is confined, and it varies with the doctor's experience. To combat this limitation, an efficient double screening technique is employed in few health care centers and hospitals by using one more specialist but, this approach is unaffordable and its time complexity is high. The research classified the thyroid nodules employing different image preprocessing techniques. Utilized histogram equalization for preprocessing in his work. The Gray-Level Co-Occurrence Matrix (GLCM) is deployed for extracting the significant features. The classification is done using ASO, k-Nearest Neighbor (KNN), and Bayesian. It is noticed that the ASO yields improved accuracy compared to KNN and Bayesian techniques.

***Keywords*---**anarchic society optimization, CAD, gray-level co-occurrence matrix, ILBP, KNN.

Introduction

Thyroid nodules constitute a generic clinical entity whose incidence rate is high. The more popular diagnosis technique that is deployed for thyroid modules is Ultrasonography. Automatic differentiation between malignant and benign thyroid nodules from ultrasound images is a remarkable improvement in assisting the practitioners in diagnosis. On the other hand, these recommendation improves the accuracy when there is a deficit of specialists. The pivotal challenge is the manner by which suitable features are extracted for this task. Several works that use diverse natural features obtained from thyroid ultrasound images have been introduced in the recent times. These using the extracted features to perform supervised classification. Literature witnesses a vast majority of works employed texture oriented features integrated with Anarchic Society Optimization classifier to perform classification or detection of nodules. This is done based on their risks in malignancy as well as for delineating the type of malignancy. If reasonable true positive rate has to be achieved, segmentation, feature extraction as well as selection and classification techniques are inevitable.

Methodology

The tremendous growth in Artificial Intelligence (AI) as well as image processing schemes are widely used in medical research. This has ultimately led to the progress of image oriented Computer-Aided Diagnosis system (CAD), that has been extensively utilized to help the doctors in diagnosing the thyroid nodules.

Preprocessing using Weighted Adaptive Median Filter

This section explains the resizing of the image that is presented as input by nearest- neighbor method. In this method, each pixel is substituted with different pixels belonging to the same color. Thus the resulting image is magnified or bigger in size than the normal image. This also preserves all the actual details. To reduce the image size when different pixels of the same color are removed, the resultant image is lesser in size compared the actual image. After determining the noise as well as the size of the filtering window, image is segmented into two types of points namely: noise and non-noise points. In non noisy points the gray values are distinguished but not filtered out. These points are discarded by applying a novel weighted median filter.

1. Determine the middle pixel of non-noisy points that is present in the filtering window.
   Median $(FW_{m,n}) = Mid\{f(m + s, n + t)\}$
   Here the terms $s, t \in [-l, l]$ as well as pixel point (m+s, n+t) indicates the non-noise point.
2. Accumulate the sum of weighted coefficients of the underlying non-noisy points denoted as (m+s, n+t)
   $sum = Median((FW_{m,n}) - f(m+s,n+t)$
3. Compute weighted coefficient of pixel point at coordinates (m + s, n + t)
   The computed output of filter is got. This is employed for substituting gray value f(m, n) of a particular noisy point (m, n) that ensures that value g(m, n) of the filter will not form any noisy point

when weighted central value namely the f(m, n) is technically equivalent to Min($P_{M\times N}$)

Localized Region based Active Contour for Segmentation

Segmentation is commonly used in clinical use of ultrasound images. This depends on localized region that depends on active contouring method. Though this method is simple and easy, the internet noise formed by speckles as well as the texture cannot be eliminated in ultrasound images. It also allows the foreground as well as background to be distinguished in the context of smaller localized sites or regions, thus discarding the presumption that representation of foreground as well as background can be performed through the collected global statistics. The assessment of these local areas eventually results in development of group of local energies at each point that is along the course of the curve. For the sake of optimizing the local energies, each point is picked separately and attempts to mitigate the energy computed in the local area. For estimating the local energies, the local neighborhoods are bifurcated into local interior and exterior. This computed energy is optimized by deploying a learning model to each local area.

Improved Local Binary Pattern (ILBP) for better Feature Extraction

An Improved Local Binary Patterns (ILBP) is proposed as gray-scale oriented texture descriptor. The indifference to lighting conditions can find the internet micro-elements present in the given image. The basic LBP is for any pixel(p_c) is given as

$$LBP\ (p_c) = \sum_{k=0}^{P-1} 1(I(p_k) - I(p_c)).\ 2^k$$

The term I(p) indicates the represents the pixel intensity. This always adheres to total count of pixels in selected proximity from the center pixel (p_c) . The local entropy of the so obtained optimal image is is computed through ridge entropy. This method computes the torsion along with consistency of the inherent ridges. Hence, the method of ILBP is employed to form a whole representation of image feature that is extracted from the images.

$$ILBP_{P,R} = \sum_{p=0}^{P-1} s(g_p)2^P + LBP_{image}$$

The term g_p indicates gray values that are uniformly located in the shape of a circle whereas gc denotes gray value of middle or center pixel along the neighborhood of size (P) with radius (R). This method is greatly enhanced by LBP_{finger}. The proposed ILBP aids in matching pairs of minutiae in ridges along with valleys, form which exact location can be found. The minutiae matched are actually marked as validated. Whereas the invalid minutiae is analyzed one more time during third recursion. This has two chances: eliminated to be random minutiae or render some useful information.

Classification using the Anarchic Society Optimization Algorithm

The Anarchic Society Optimization (ASO) is deployed as a classifier. The features extracted are provided to ASO algorithm in the form of input. ASO is a novel mechanism among swarm-intelligence technique. The discussed ASO algorithm attempts improving the classification performance. At first, few community members (features) are chosen in random within the confined solution space. The fitness of every member is determined. Depending on estimated fitness value and also by comparing with the term $X^*(k)$, the measures like P^{best} as well as G^{best}, the movement rule and new position respectively, will be determined. Once sufficient numbers of iterations are over, at least one of the members will attain the ideal position.

Movement Policy Based on present Positions

The initial movement policy pertaining to i^{th} member in k^{th} iteration $[MP_i^{current}(k)]$ is computed based on current position. The Fickleness Index $(FI_i(k))$ of member (i) in a specified iteration (k) is useful in selecting the movement. This index indeed renders a satisfaction measure of present position of i against other members. It is always favorable to select the pertaining movement policy based on $X^*(k)$. Otherwise, i displays a completely random and surprise movement.

$[MP_i^{current}(k)]$ = moving towards $X^*(k)$ $0 \le FI_i(k) \le \alpha_i$ moving towards a random value $X_i(k)$ $\{\alpha_i \le FI_i(k) \le 1\}$

Movement Policy Based on Positions of Other Members

The next movement policy for member i belonging to iteration k $[MP_i^{society}(k)]$ is designed based on positions other members. All members should move along G^{best}. Then it becomes is very difficult to foresee the movement of the members because of its anarchist characteristics. Sometimes the members move towards some other community also. The external irregularity index $(EI_i(k))$ for i belonging to iteration k is found through:

$$EI_i(k) = 1 - e^{-\theta_i [f(X_i(k)) - f(G(k))]}$$

$$EI_i(k) = 1 - e^{-\delta_i D(k)]}$$

The term which θ_i as well as δ_i refers to positive numbers. The value D(k) is dispersion measure like coefficient of variation indicated as CV(k). The above expression denotes the distance between i and Gbest. If the distance is small, then it exhibits logical behavior. Otherwise, a disorderly behavior can be noticed. Apart from this, the above expression also represents a good diversity index within the community that has a direct relation with group's versatility. If the index is selected, then the members of the group will act more sensibly, thus their diversification will also be less. Hence, by considering a threshold for the term $EI_i(k)$, the underlying movement policies that relies on locations of other members can be determined. As the threshold approaches to zero, more randomness can be

expected with the members. If the threshold reaches to one, then members would behave sensibly.

Movement Policy Based on Previous Position

The third movement policy for the member i belonging to iteration k [$MP^{past}(k)$] is found from the earlier positions. To select this policy, the position of member i in iteration k and Pbest is compared. If the member is proximal to P^{best}, the member behaves sensibly. In other case, the member will behave without any logic. To find member movement based on previous positions, an internal irregularity index (II_i (k)) is given as: $II_i(k) = 1 - e^{-\beta i\ [f(X_i(k))-f(P_i(k))]}$

The value bi is a positive number. The selection of threshold for IIi(k), for the third movement policy is found as below:

$$MP_i(k)] = \begin{cases} \text{Previous movement towards } P^{best} & 0 \le II_i(k) \le tres\ old \\ \text{member i moving toward a random } X_i & (k)t\ res\ old \le II_i(k) \le 1 \end{cases}$$

As the threshold comes closer to zero, the movements would also be random. If the threshold comes closer to unity, then members will exhibit sensible movement.

Combination of the Movement Policies

For selecting the final policy, all the policies that are described above are integrated. After computing the movement policies, all the members must combine these policies and move to new position. One simple way to converge or integrate them is select them with the optimal or best answer. Alternatively, the policies can be concatenated one after another to form a sequential combination. Crossover technique can also be used for handling continuous problems that are encoded as and can be deployed in a sequence to merge the policies.

The classification of ultrasound imageis done ASO algorithm based on the fitness function. It eventually produces an elevated True Positive (T_p) for the pertaining thyroidimage dataset.

Results and Discussions

The experimental analysis is done in matlab with 400 .jpeg images of size 256 × 256. Some of the contemporary schemes such as Multilayer perceptron (MLP) are compared with ILBP-ASO.

Table: Performance Comparison

	Performance metrics in (%)				
Methods	Accuracy	Precision	Recall	F-measure	Specificity
Histogram	89	86	81	83	81
MLP	91	89	85	86	84
ILBP-ASO	96	92	89	90	92

Accuracy

Classification accuracy is rated as correctness of the developed model. It is estimated as the fraction of actual classification $(T_p + T_n)$ and aggregate of all the parameters $(T_p + T_n + F_p + F_n)$. It is given as:

$$\text{Accuracy} = \frac{T_p + T_n}{(T_p + T_n + F_p + F_n)}$$

The term T_P is count of right predictions whereas T_n is the count of incorrect predictions. F_p denotes the count incorrect predictions of any instance being negative whereas F_n is vice versa.

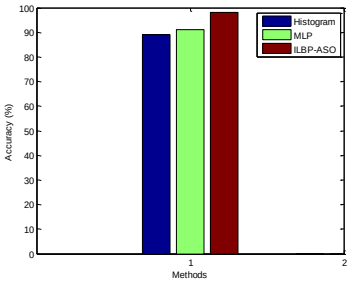

Figure 4.1: Comparison of Accuracy

The graph shown in figure 4.1 displays accuracy comparison. It is evident that proposed technique has improved accuracy than its peers. These results assures that the proposed ILBP-ASO has 96% of accuracy which is higher than MLP and histogram.

Precision

This metric is the share of T_p and sum of the T_p and T_n. This is give as:

Precision(P) = $\frac{T_p}{T_p+F_p}$

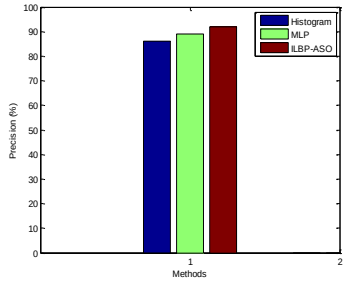

Figure 4.2: Precision Comparison

The graph in the above figure 4.2 depicts the precision metric comparison for the techniques. The result of experiments proves that the proposed ILBP-ASO

algorithm yields 92% of precision while histogram and MLP techniques achieves 86% and 89% correspondingly.

Recall

Recall is computed based on the data retrieval based on its T_p and T_n forecast. It is expresses as:

$$\text{Recall(R)} = \frac{T_p}{T_p + F_n}$$

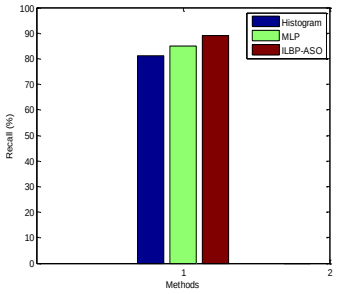

Figure 4.3: Recall Comparison

The graph in the above figure 4.3 exhibits that the comparison of recall for the given techniques. It is evident that the proposed scheme produces improved recall that other two techniques. The techniques areplotted along the x-axis. The recall values are plotted along y-axis. These results assures that the proposed ILBP-ASO algorithm yields 89% of recall while the histogram and MLP techniques yield 81% and 85% correspondingly.

F-Measure

This is a direct implication of the accuracy. It is estimated as the geometric mean of precision and recall.

$$\text{F1 Score} = 2 * \frac{\text{Recall} * \text{Precision}}{(\text{Recall} + \text{Precision})}$$

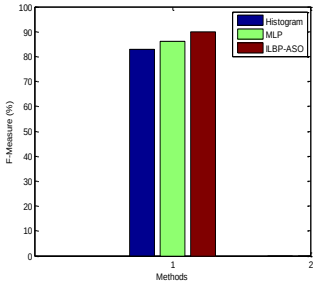

Figure 4.4: F-Measure Comparison

Figure 4.4 shows the comparison of F-measure. It is clear that that proposed method shows better F-measure than the histogram as well as MLP. The result of

the experiments corroborates that ILBP-ASO yields 90% of F-measure while histogram and MLP techniques attain 83% and 86% respectively.

Specificity

This is a metric that assess the fraction of negatives, that are correctly classified.

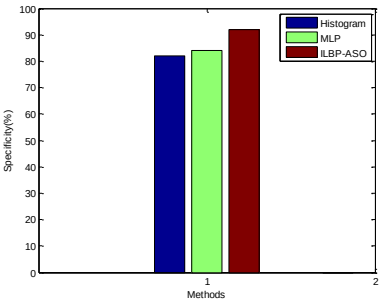

Figure 4.5: Specificity Comparison

The specificity of the discussed ILBP-ASO approach is compared with the contemporary techniques like histogram and MLP. The ILBP-ASO technique yields 92% of specificity while other techniques like histogram and MLP yields 81% and 84% correspondingly.

Conclusion

Ultrasound imaging is popularly deployed in hospitals for investigating the nodules present in thyroid images. This work introduces ILBP-ASO for the improvement of the thyroid image classification outcomes. The preprocessing is performed using weighted adaptive median filters that elevates the accuracy. Next, the ILBP is employed for extracting the features from Ultrasound images. ASO can be further used to improve theaccuracy. The experimental result portrays that proposed technique produces better classification accuracy, recall, precision, specificity and f-measure than histogram and MLP techniques.

Future Work

The iterative filter can be developed on the basis of the local statistics to eliminate the speckle noise with no effect on the structural components of the image

References

1 Acharya, U.R, Faust, O, Sree, S.V, Molinari, F and Suri, J. S, (2012). ThyroScreen system: high resolution ultrasound thyroid image characterization into benign and malignant classes using novel combination of texture and discrete wavelet transform. Computer methods and programs in biomedicine, vol. 107, no. 2, pp.233-241.

2 Agarap, A.F, (2017). An architecture combining convolutional neural network (CNN) and support vector machine (SVM) for image classification, pp. 1-4.

3 Ahmadi-Javid, A, (2011). Anarchic Society Optimization: A human-inspired method. IEEE congress of evolutionary computation (CEC), pp. 2586-2592.
4 Albawi, S, Mohammed, T.A and Al-Zawi, S, (2017). Understanding of a convolutional neural network. International Conference on Engineering and Technology (ICET), pp. 1-6.
5 Almufti, S.M, (2019). Historical survey on metaheuristics algorithms. *International Journal of Scientific World*, vol. 7, no. 1, pp.1-12.
6 Bibicu, D, Moraru, L and Biswas, A, (2013). Thyroid nodule recognition based on feature selection and pixel classification methods. *Journal of Digital Imaging*, vol. 26, no. 1, pp.119-128.
7 Bozorgi, A, Bozorg-Haddad, O and Chu, X, (2018). Anarchic society optimization (ASO) algorithm. In Advanced Optimization by Nature-Inspired Algorithms, pp. 31-38.
8 Buddhavarapu, V. G, (2020). An experimental study on classification of thyroid histopathology images using transfer learning. Pattern Recognition Letters, pp. 1-9.
9 Carraro, R, Molinari, F, Deandrea, M, Garberoglio, R and Suri, J.S, (2008). Characterization of thyroid nodules by 3-D contrast-enhanced ultrasound imaging. Annual International Conference of the IEEE Engineering in Medicine and Biology Society, pp. 2229-2232.
10 Cesareo, R, Palermo, A, Pasqualini, V, Manfrini, S, Trimboli, P. Stacul, F and Bernardi, S, (2020). Radio frequency ablation on autonomously functioning thyroid nodules: A critical appraisal and review of the literature. Frontiers in Endocrinology, pp. 1-6.
11 Chang, C.Y, Hong, Y. C and Tseng, C.H, (2011). A neural network for thyroid segmentation and volume estimation in CT images. IEEE Computational Intelligence Magazine, vol. 6, no. 4, pp. 43-55.
12 Chen, N, Klushyn, A, Kurle, R, Jiang, X, Bayer, J and Smagt, P, (2018). Metrics for deep generative models. International Conference on Artificial Intelligence and Statistics, pp. 1540-1550.
13 Chi, J, Walia, E, Babyn, P, Wang, J, Groot, G and Eramian, M, (2017). Thyroid nodule classification in ultrasound images by fine-tuning deep convolutional neural network. *Journal of Digital Imaging*, vol. 30, no. 4, pp.477-486.
14 Cho, S.J, Baek, J.H, Chung, S.R, Choi, Y.J and Lee, J. H, (2020). Long-term results of thermal ablation of benign thyroid nodules: a systematic review and meta-analysis. Endocrinology and Metabolism, vol. 35, no. 2, pp. 339-350.
15 Dash, S and Senapati, M. R, (2018). Gray level run length matrix based on various illumination normalization techniques for texture classification. Evolutionary Intelligence, pp.1-10.
16 Ding, J, Cheng, H. D, Huang, J and Zhang, Y, (2014). Multiple-instance learning with global and local features for thyroid ultrasound image classification. IEEE International Conference on Biomedical Engineering and Informatics, pp. 66-70.
17 Ding, J, Cheng, H.D, Huang, J, Zhang, Y and Ning, C, (2011). A novel quantitative measurement for thyroid cancer detection based on elastography. IEEE International Congress on Image and Signal Processing, vol. 4, pp. 1801-1804.
18 Dogantekin, E, Dogantekin, A and Avci, D, (2011). An expert system based on generalized discriminant analysis and wavelet support vector machine for

diagnosis of thyroid diseases. Expert Systems with Applications, vol. 38, no. 1, pp. 146-150.
19 Dorigo, M and Stützle, T, (2019). Ant colony optimization: overview and recent advances. Handbook of Metaheuristics, pp. 311-351.
20 Frannita, E. L, Nugroho, H.A, Nugroho, A and Ardiyanto, I, (2018). Thyroid Nodule Classification Based on Characteristic of Margin using Geometric and Statistical Features. IEEE International Conference on Biomedical Engineering (IBIOMED), pp. 54-59.